External Tank Chill Effect on the Space Transportation System Launch Pad Environment

R. A. Ahmad* and S. Boraas†
Thiokol Corporation, Brigham City, Utah 84302

The external tank (ET) of the Space Transportation System (STS) contains liquid oxygen and liquid hydrogen as oxidizer and fuel for the Space Shuttle main engines (SSMEs). Once the cryogens have been loaded into the ET, the temperature of the air surrounding the STS is chilled by the cold outer surface of the ET. This paper describes a two-dimensional flow and thermal analysis to determine this chill effect on the STS launch pad environment subsequent to the ET loading operation. The analysis was done assuming winter conditions and a northwest wind direction. An existing CFD code, Parabolic Hyperbolic Or Elliptical Numerical Integration Code Series (PHOENICS '81), was used in the study. The results are presented as local and average values of the heat transfer coefficient, the Nusselt number, and the surface temperature around the redesigned solid rocket motors (RSRMs) and the ET. The temperature depression caused by the ET chilling of the air in the vicinity of the RSRMs was calculated to be 3°F below the ambient. This compares with the observed 1–2°F RSRM surface temperature depression based upon measurements made prior to the winter flight of STS-29. Since the surface temperature would be expected to be slightly higher than the local air temperature, the predicted temperature depression of the air appears to be substantiated.

Nomenclature

D = diameter of the RSRM (12.2 ft) or the ET (28 ft)
$F_{s\text{-sky}}$ = view factor of the RSRM or the ET to the sky (0.5)
G = thermal conductance of the RSRM or the ET, Btu/h-ft^2-°F
h = convective heat transfer coefficient, Btu/h-ft^2-°F
$\bar{h}_l, \bar{h}_u$ = lower and upper limits on the average heat transfer coefficient, Btu/h-ft^2-°F
$\bar{h}_m$ = mean value of the average heat transfer coefficients, Btu/h-ft^2-°F
h_r = radiative heat transfer coefficient, RSRM or ET to the sky, Btu/h-ft^2-°F
k_f = thermal conductivity of air, 0.013 Btu/h-ft-°F
$k\epsilon$ = turbulence kinetic energy, ft^2/s^2
K = statistical variable dependent upon the population size
n = population size
Nu_D = Nusselt number (hD/k_f)
Pr = Prandtl number
Re_D = Reynolds number ($U_\infty D/\nu$)
t = half the thickness of the adjacent cell to the surface
T = temperature, °F
U_∞ = freestream wind velocity, ft/s
y, z = Cartesian coordinates (Fig. 2)
ϵ = emissivity of the RSRM (0.9)
ϵp = rate of dissipation of turbulence kinetic energy, ft^2/s^2
ν = kinematic viscosity of air (0.4565 ft^2/h)
σ = Stefan-Boltzmann constant (0.1714×10^{-8} Btu/h-ft^2/°R^4)
σ' = population or biased standard deviation
θ = angular direction, deg (Fig. 3)

Subscripts

a = local ambient in the vicinity of the STS
cell = finite volume adjacent to a wall
D = based on diameter
d = depression ($T_\infty - T_{a,\min}$)
f = fluid
fsp = forward stagnation point
i = inside
min = minimum
NC = natural convection
o = outside
rad = radiation
s = surface
sky = sky temperature
∞ = freestream conditions

Superscript

$-$ = average

Received Dec. 21, 1989; revision received June 1, 1990; accepted for publication Sept. 23, 1990.

*Associate Scientist, Aero/Thermal Section; currently, Associate Scientist, Engineering Analysis Department. Member AIAA.
†Supervisor, Aero/Thermal Section. Senior Member AIAA.

Introduction

THE external tank (ET) of the Space Transportation System (STS) contains 146,000 gal of liquid oxygen and 393,000 gal of liquid hydrogen as oxidizer and fuel for the Space Shuttle main engines (SSMEs). The loaded ET has a chilling effect on the STS launch pad environment. To determine this effect requires that the STS adjoining flowfield be known with sufficient accuracy so that accurate heat transfer coefficients can be determined at the STS component surfaces. This chilling effect has been studied,[1-5] but, in each of these instances, the coefficients have been estimated since the exact flowfield was unknown. The purpose of this study was to obtain a more accurate assessment of the chilling effect through the use of more accurate heat transfer coefficients since coefficients found in literature are generally inappropriate for the low wind/large multiple cylinder configuration typified by the STS on the launch pad. Thus the coefficients were obtained from a more exact two-dimensional calculation of the flow/thermal field using the STS geometry and the PHOENICS '81 flow/thermal code.[6,7]

The flow/thermal field was calculated in a plane parallel to and through a slice between two planes perpendicular to the STS longitudinal axis and passing through the lower portions of the redesigned solid rocket motors (RSRMs), the ET, and the wing of the Orbiter as shown in Fig. 1. The flow was generated by a wind from the northwest direction, a condition which frequently prevails in winter at the launch site. Results from this two-dimensional PHOENICS '81 solution were first

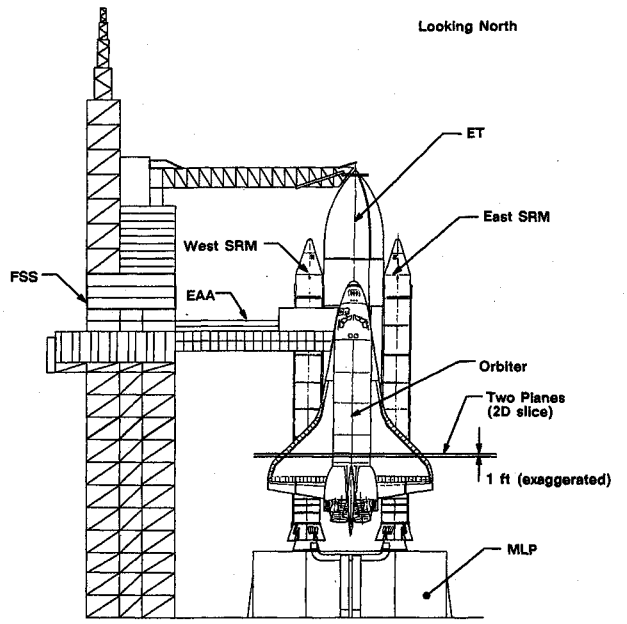

Fig. 1 STS on the launch pad.

used to provide accurate boundary conditions for a three-dimensional Global Thermal Model (GTM), which had been developed for use during the RSRM redesign. Results also provided accurate coefficients for use in the design of the heaters for the RSRM case joints and igniter, in the determination of the required temperature conditioning of the region between the RSRM aft skirt and nozzle, and in the prediction of the RSRM propellant mean bulk temperature (PMBT). In this study, the solution provided the necessary flow/thermal information where the thermal field was solved by using a forced convection heat transfer mode. The local and average values of the heat transfer coefficient, the Nusselt number, and the wall temperature around the RSRMs and the ET were calculated along with the temperature depression of the air, relative to the ambient, in the vicinity of the STS. Since polar coordinates could not be used because of the complex geometry, a Cartesian system with stepped walls was used.

Future improvements in the determination of these coefficients will include the chilling effect of the downdraft produced by the purged gaseous oxygen (GOX) from the top of the ET. This should make for an even more precise prediction of the temperature depression and the STS surface component temperatures.

Previous Studies

The STS launch configuration was first modeled thermally by SRS Technologies[1] for the solid rocket motor (SRM) where the emphasis was placed on evaluating the temperatures of the lower right SRM segment during a period of several hours before launch and after completion of the ET tanking operation. In that study, the heat transfer coefficient around the SRM was selected to be in the range of 0.5 to 4 Btu/h-ft^2-°F for wind speeds of 0–20 mph and sky temperatures of -15 to -30°F. The minimum SRM surface temperature at launch was determined to be 27°F for an ambient temperature of 23°F, a sky temperature of -15°F, a wind speed of 10 mph, and an assumed forced convection heat transfer coefficient of 2 Btu/h-ft^2-°F. At the same time, the ET surface temperature was determined to be at -29.5°F assuming a natural convection heat transfer coefficient of 0.98 Btu/h-ft^2-°F. For these conditions, the temperature depression of the air adjacent to the ET was found to be 5.5°F.

In an earlier study, Singhal et al.[2] had determined the feasibility of using hot-gas jets to prevent prelaunch ice formation on the ET. In that study, the PHOENICS code adequately modeled the three-dimensional jet/ambient thermal environment. The results of this analysis, which dealt with heating of the air adjacent to the ET and the SRMs to a temperature as much as 100°F warmer than ambient, provided neither information nor insight into its cooling as a result of being in contact with the cold ET surface.

Bachtel[3] summarized the results of some two- and three-dimensional analyses conducted during the STS-51L investigation period to determine the maximum subcooling at the SRM and the ET surfaces. These results showed that at the SRM surface, the subcooling could be as much as 1.5–5.5°F; the latter being the value determined by SRS Technologies.

Rockwell International (RI),[4] in its latest version of the Thermal Interfaces Design Data Book (TIDDB), has provided prelaunch surface temperature histories of the Space Shuttle components on the launch pad for a cold day environment and after completion of the ET tanking operation. The surface temperatures at the lower portions of the SRMs, which correspond to the slice considered in this study, are given as a function of time starting at 70 h prior to launch. The temperatures were determined to be in the range of 16 to 40°F, for a 38°F ambient temperature. Thus a maximum surface temperature depression of 22°F could be expected as a result of ET chilling. Mongan,[5] in a related RI study, showed that the local air temperature adjacent to the SRM surface could be as much as 16°F less than the ambient for a quiescent or no wind condition. This temperature differential was shown to decrease rapidly with increasing wind speed as a result of increased mixing of the local chilled air with the ambient.

Present Study

In all of the previous studies, the appropriate heat transfer coefficients were estimated since the actual three-dimensional flowfield was not known. In this study, the PHOENICS '81 code was used to determine a more exact flowfield of the STS launch pad environment and consequently more exact heat transfer coefficients. These permitted a more precise calculation of the ET chill effect in terms of the local air temperature depression and RSRM surface temperatures. The governing equations within PHOENICS '81, the numerical model, and the boundary conditions used in the present study are discussed in the remainder of this section.

Governing Equations

The PHOENICS '81 is an accepted industry-wide multidimensional computational fluid dynamics and heat transfer computer code[6,7] that has been used extensively in the aerospace industry for a variety of applications. The code uses a fully conserved and implicit formulation to solve the Navier-Stokes equations. The conservation of phase-mass, momentum, energy, chemical species, and other fluid properties are all expressed in PHOENICS '81 by the general partial differential equation[6,7]

$$\partial/\partial t(r_i\rho_i\phi_i) + \mathrm{div}(r_i\rho_i v_i\phi_i - r_i\Gamma_{\phi i}\mathrm{grad}\phi_i) = r_i\, S_{\phi i} \qquad (1)$$

where ϕ_i is the ith component of the conserved property ϕ, r_i and ρ_i are the volume fraction and density of ϕ_i, and where $\partial/\partial t(r_i\rho_i\phi_i)$, $\mathrm{div}(r_i\rho_i v_i\phi_i)$, and $\mathrm{div}(r_i\Gamma_{\phi_i}\mathrm{grad}\phi_i)$ denote, respectively, its transience, convection, and diffusion. The term $\Gamma_{\phi i}$ is the exchange coefficient for ϕ_i and $S_{\phi i}$ defines its source(s).

The partial differential equation for each of the conserved quantities is converted to a finite difference form using a staggered grid and upwind differencing scheme that embodies finite-domain formulation. Integration of the partial differential equations led to a set of finite domain equations (FDEs), one for each conserved quantity, which were solved by PHOENICS '81 in an iterative manner because of their nonlinearity. PHOENICS '81 has the flexibility to represent solid obstructions in the flowfield by the blockage concept.

The heat conductances through the composite walls of an STS component were calculated assuming one-dimensional conduction heat transfer. Using the thicknesses (x_j) and thermal conductivity (k_j) of each jth layer of a composite wall, the heat conduction (q''_{cond}) through n layers was calculated from

$$q''_{cond} = \sum_{j=1}^{j=n} (T_i - T_s)/(x/k)_j \qquad (2)$$

where T_i is the inner surface temperature of the inner layer, and T_s is the temperature at the outer surface. In this study, the inner temperature T_i of the RSRM wall was the PMBT, while that inside the ET was assumed to be that of liquid hydrogen.

Numerical Model

The primary task in this study was the determination and the analysis of the two-dimensional flow/thermal field generated by a northwest wind in a plane parallel to and passing through the two-dimensional slice of the STS as shown in Fig. 1. The generation of this field assumed the flow to be steady, turbulent, and elliptic.

Figure 2 shows the two-dimensional solution domain used in the determination of this field. The domain had a highly nonuniform grid to permit a better resolution in the areas of interest. The two-dimensional domain (115×65 ft), which contains the STS components, was divided into 138×73 cells in the y and z directions, respectively, for a total of 10,074 cells. This is more than twice the number of cells (4224) used in the three-dimensional study of Ref. 2; consequently, it provided a good resolution near the ET surface.

A Cartesian coordinate system with stepped walls was used in this study as it had been done in an earlier study[2] of the Space Shuttle environment. Although body-fitted coordinates (BFC) were available, they were not being widely used at the time this study was initiated. The choice of a Cartesian system also allowed for ease of setup and computational economy although the BFC coordinates would have provided greater accuracy in the heat transfer results. It would appear that the use of stepped walls to approximate oblique walls might lead to inaccuracies as a result of recirculation zones forming within the steps. However, in the present study, the grid was too coarse to resolve the detail around the steps, and consequently the solution procedure simply "sees" the inclined wall. This stepped procedure does not prevent useful results from being obtained especially in situations where the flow is not dominated by wall shear. Furthermore, in a supporting investigation where the method of partial porosity was used to represent the RSRM surface more accurately, it was shown that the quality of the solution was not improved.

The flow around the STS components in this problem involves the convection of scaler quantities along a direction that is not aligned with the y or z directions. When this situation arises, numerical schemes will give rise to a phenomenon known as numerical diffusion (false diffusion). This can be minimized through a more accurate interpolation of a flow variable between nodal points and/or through the use of a finer grid. PHOENICS '81, with its built-in schemes, achieves this increased accuracy in interpolation. Special attention was also given to the selection of a grid to further reduce the effect of this diffusion.

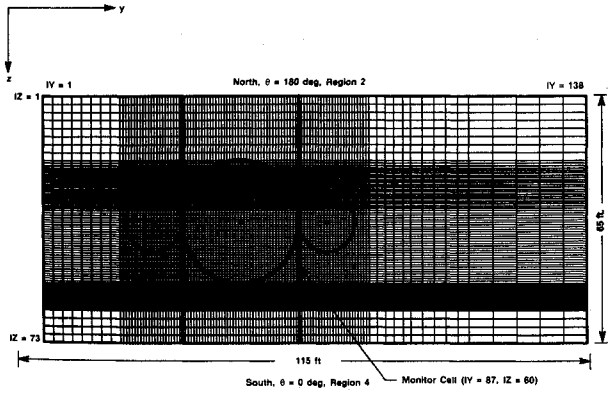

Fig. 2 Two-dimensional computational grid of the STS components.

The final size of the computational domain had been determined in an earlier study[8] where starting from a small grid the number of grid points was gradually increased until grid independent results were achieved. Several grid sizes were examined before choosing the final grid of 138×73 cells. In the case of a smaller grid (118×69), a laminar flow generated by a west wind produced a wake on the downstream side of the east RSRM, which resulted in nonuniform flow at the outlet. The domain was then increased to its final size by increasing the number of cells in the wake region and adding a region to the south side of the Orbiter. The laminar flow case was then rerun, and the results demonstrated that the flow was now uniform after 300 sweeps and fully converged after 700 sweeps. Repeating the above calculations indicated that 1000 sweeps would be required for convergence whenever the flow is turbulent.

The convergence of a solution is generally achieved by monitoring a cell within a region of the flow that is of particular interest, either from an engineering standpoint or because convergence difficulties are expected within that region. The procedure for doing this in PHOENICS '81 is described in Refs. 6 and 7.

Boundary Conditions

The requirements complied with and the boundary conditions used in this analysis are as follows.

1) The study complied with the requirements of Contract End Item Specification No. CPWI-3600A[9] but did not account for rainfall or ozone in the launch pad area.

2) The northwest wind speed of 58 ft/s satisfied the maximum wind speed requirement of Ref. 10. The direction of the wind was 30 deg south of north. This was considered to be a typical wind direction for the winter months at the Kennedy Space Center launch site.

3) The assumed ambient temperature of 15°F was conservative because it was much lower than that expected during a winter launch. The effective sky temperature[4] was assumed to be −30°F.

4) The temperature of the air in the RSRM cavity or motor bore was assumed to be that of the PMBT. At 52°F, this was the coldest PMBT ever experienced.[11]

5) The temperature at the inner boundary of the ET for the fuel tank was assumed to be that (−423°F) of liquid hydrogen.[12]

6) The view factor of the RSRM to the sky was assumed to be 0.5.

7) The thermal radiation exchange between the RSRM and the ET was not included because the capability of calculating view factors with a code such as FACET was not available at the time.

8) The mass flow rate, velocity, enthalpy, turbulence kinetic energy, and its rate of dissipation were applied as input boundary conditions along the domain's inlet regions 1 and 2 (Fig. 2).

9) The outlet boundaries along regions 3 and 4 were treated as constant pressure boundaries; that is, fluid was allowed to enter or exit depending on the local calculated difference between the near-boundary grid pressure and the ambient pressure.

10) The surface of the Orbiter was assumed to be adiabatic.

11) Turbulence effects were accounted for by using the two-equation ($k\epsilon$-ϵp) turbulence model.

The conservative assumption made in the selection of an ambient temperature of 15°F and the assumed 30-deg direction for the northwest wind was expected to result in the most severe ET chilling effect.

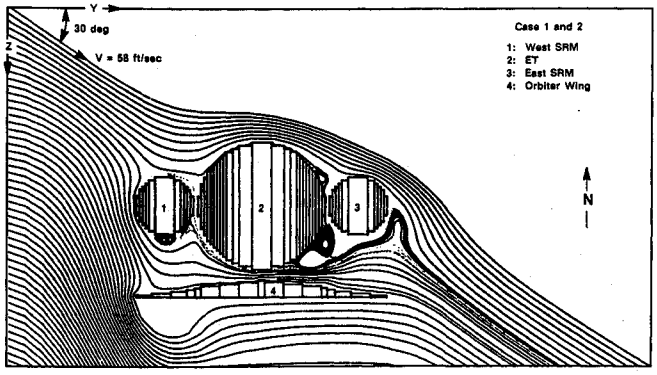

Fig. 3 Two-dimensional streamlines around the STS components.

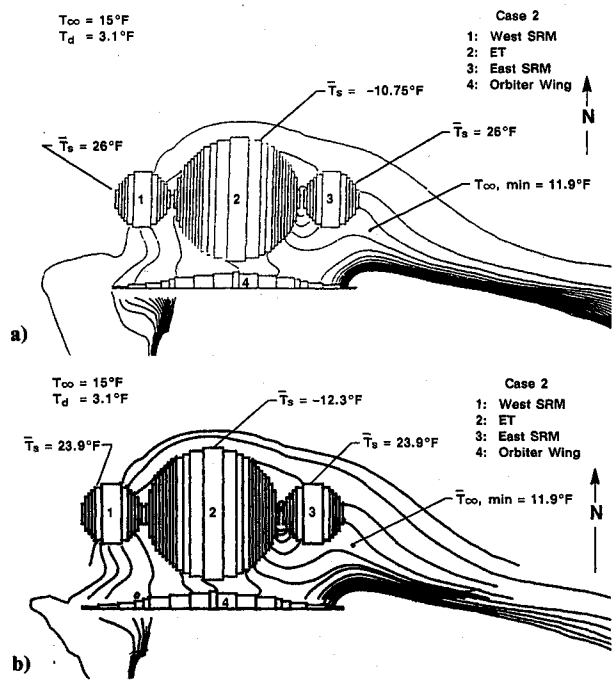

Fig. 4 Isotherms around the STS components.

Results

The numerical model and the imposed boundary conditions were used to make two calculations of the flow/thermal field surrounding the STS components (RSRMs, ET, Orbiter). The first of these was conducted without thermal radiation to the sky; the second considered radiation. The inner temperatures of the RSRMs (52°F) and the ET (−423°F) along with that of the sky (−30°F) and the ambient (15°F) served as thermal drivers. With heat conduction considered through the walls of the ET and RSRMs and heat convection at their outer surface, the flow/thermal analyses were truly conjugate.

Because of the concern with flow convergence within the wake of the ET, a monitor cell was chosen to lie on the leeward side of the ET. Identified by cell number IX = 1, IY = 87, and IZ = 60, this cell is shown in Fig. 2. Calculations of the flow variables (enthalpy, velocity, pressure, turbulence kinetic energy, and its rate of dissipation) within the entire two-dimensional domain were made by monitoring the same variables in the monitor cell during repeated sweeps until convergence was reached. Results of some of these calculations, such as the streamlines around the STS components as shown in Fig. 3, are common to both cases. These streamlines are shown to adjust to the presence of the STS components. Several vortices appear; the largest is on the east side of the ET in the expansion region downstream of the vena contracta between the ET and the Orbiter wing. This flowfield compares very well with the results of a similar but later study at RI.[13]

Case 1: Without Thermal Radiation to the Sky

In this case, radiation exchange between the STS component surfaces and the sky was not considered. Figure 4 shows the computed isotherms in the vicinity of the STS components. The maximum and minimum air temperatures were found to be $T_{max} = 15°F$ and $T_{min} = 11.9°F$; the latter represents a 3.1°F temperature depression relative to the 15°F ambient. The average surface temperatures of the west RSRM, the east RSRM, and the ET were calculated to be 26, 26, and −10.8°F, respectively. Reference 10 states, "Once External Tank loading has been initiated, the temperature of the air surrounding the other shuttle elements is affected by chilling from the cold surface of the External Tank and from the SSME drain purges and, for the cold day case, the combined effect can be up to 5 degrees Fahrenheit colder than the ambient air temperature." It should be noted that the 5°F temperature depression quoted here is the same value noted earlier[1,3] and is based on a natural convection boundary layer along the ET. The above computed value of 3.1°F for the temperature depression is slightly more than half of the above quoted value and represents a reduction in the natural convection value as a result of mixing the local chilled air with the warmer ambient air due to the influence of the northwest wind.

Since the present study dealt with forced convection, a comparison was made with the forced convection results of the analysis conducted by RI.[13] In that study, surface temperatures of 0, 10, and 25°F were specified for the ET, while the surfaces of the SRMs were assumed to be adiabatic and at the ambient temperature of 38°F. Thermal radiation to the sky was not considered but different wind directions were assumed. RI concluded from their results, based upon their computational domain of 3007 cells, that a northwest wind would produce the maximum ET cooling effect on the east RSRM. This confirmed what had been assumed in this study. In the same RI document, a conclusion was made that stated, "Although the combined probability of low wind speed and low ambient temperature is rare (References 6.13 and 6.14), a temperature depression of more than 10°F was calculated at 1 knot West wind conditions and can occur."

The local surface temperature of either RSRM or the ET was calculated from an energy balance between the fluid cell adjacent to a surface and the surface:

$$T_s = [(k_f/t)T_{cell} + GT_i]/[(k_f/t) + G] \quad (3)$$

Figure 5a shows the local surface temperature around the east and west RSRM as a function of the angular coordinate. Due to the temperature scale used, temperature variations are not as large as they might appear. Figure 5b gives the variation of the surface temperature around the ET. The maximum temperature variation in the angular direction for either RSRM and the ET is 1.6°F. Reference 14, in a report on the Challenger accident, states, "It is possible that the aft field joint of the right Solid Rocket Booster was at the lowest temperature at launch, although all joints had calculated local temperatures as low as 28 ± 5 degrees Fahrenheit." The RSRM surface temperature results of this study are in agreement with this statement.

Figure 6a shows the angular variation of the heat transfer coefficient for both RSRMs and the ET. The average heat transfer coefficients around the west RSRM, east RSRM, and the ET were calculated to be 4.64, 4.69, and 4.63 Btu/h-ft^2-°F, respectively. The corresponding local Nusselt numbers around the RSRMs and those around the ET are given in Refs. 15 and 16. The average Nusselt numbers around the west RSRM, the east RSRM, and the ET were calculated to be 4075, 4120, and 9596, respectively.

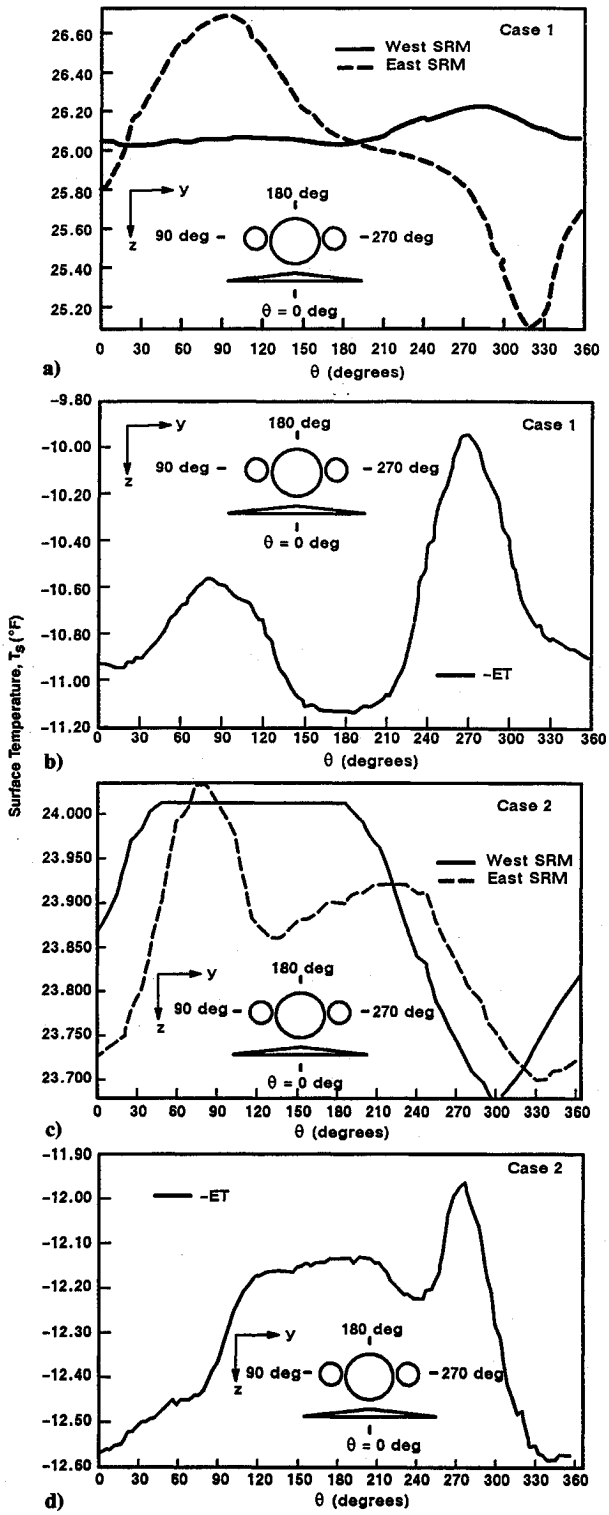

Fig. 5 Local surface temperatures around the RSRMs and the ET of the STS on the launch pad.

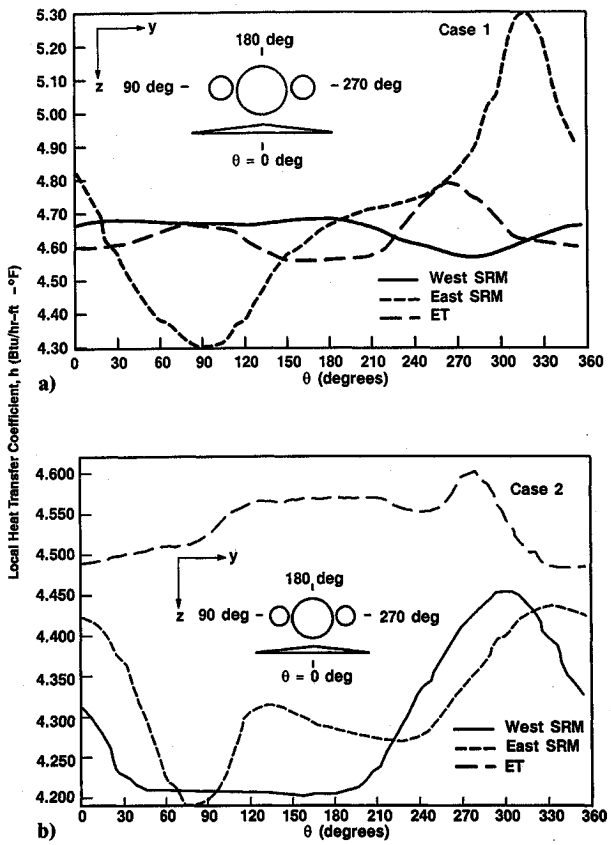

Fig. 6 Local heat transfer coefficient around the RSRMs and the ET of the STS on the launch pad.

Case 2: With Thermal Radiation to the Sky

In this case, thermal radiation exchange between the RSRM surfaces and the sky and the ET surface and the sky were included. The net radiation heat flux exchange can be conveniently expressed as

$$q''_{\text{rad}} = h_r\,(T_s - T_{\text{sky}}) \tag{4}$$

where

$$h_r = \epsilon\sigma(T_s + T_{\text{sky}})(T_s^2 + T_{\text{sky}}^2)F_{s\text{-sky}} \tag{5}$$

With these equations, the radiation has been modeled in a manner similar to convection in that the radiation flux equation has been linearized. This makes the heat rate proportional to a temperature difference rather than to the difference between two temperatures to the fourth power. This is done in compliance with the method of representing heat sources/sinks in the PHOENICS '81 code. The thermal properties were evaluated at the ambient temperature. The local surface temperature was then calculated as follows:

$$T_s = [(k_f/t)T_{\text{cell}} + h_r T_{\text{sky}} + GT_i]/[(k_f/t) + h_r + G] \tag{6}$$

The results for this case are discussed in detail in Refs. 15 and 16 and are given in Figs. 4b, 5c, 5d, and 6b. The results correspond to the results of case 1 when thermal radiation exchange to the sky was not included. They are summarized as follows:

1) The average surface temperatures of the west RSRM, the east RSRM, and the ET were calculated to be 24, 24, and −12°F, respectively. Thus radiation to the sky results in an additional temperature drop of 2°F in the average surface temperatures of the RSRMs and the ET when compared with the case 1 results.

2) The average heat transfer coefficient around the west RSRM, the east RSRM, and the ET were calculated to be 4.29, 4.32, and 4.54 Btu/h-ft²-°F, respectively. This shows a decrease in the heat transfer coefficient when radiation to the sky is considered.

3) The corresponding average Nusselt numbers around the west RSRM, the east RSRM, and the ET were calculated to be 3873.5, 3905, and 9867, respectively. These results show that Nusselt numbers on the RSRMs decreased as a result of radiation while the number for the ET increased.

4) The temperature depression in the vicinity of the STS was calculated to be 3.1°F (Fig. 4b), which is the same as that found in case 1 in the absence of radiation.

The above results show that the ET can chill the local air to about 3°F below the ambient temperature during severe winter conditions. This compares with the 1-2°F surface temperature depression on the RSRMs as determined from the ground environment instrumentation during the winter flight of STS-29. Since a surface temperature would be expected to be slightly higher than that of the local air adjacent to the surface, there appears to be an agreement between the predicted temperature depression and the STS-29 surface temperatures. Differences between the two values may have been the result of other factors. First, the ambient temperature used in the present PHOENICS '81 prediction was much colder than the actual launch temperature of STS-29. Second, the two-dimensional PHOENICS '81 solution is only a partial representation of the three-dimensional flow in the STS environment. These and possibly other factors could explain the difference.

Comparison with Other Studies

The two-dimensional cross-sectional slice through the STS resulted in a fairly complex configuration. In the literature, there are numerous expressions for free and forced convective heat transfer. Generally they apply to simple geometries such as plates, cylinders, or banks of cylinders as in the case of heat exchangers. In addition, these studies have been conducted for comparatively small geometries and certainly not for components of the size used in the STS. Since heat transfer is believed to be dependent upon component size and since this information was also lacking for large independent components when these are arranged as in the STS, the need for the present study was obvious. Despite these differences, it was desirable to compare the current results with those in the previously reported studies. Since the STS geometry is more complex than a single cylinder, the best comparison was believed to be the average value of the heat transfer coefficient. This comparison was made for the west RSRM, since the northwest wind impinges directly upon this motor. In addition, a comparison was made based on the forward stagnation point heating on the west RSRM. These comparisons are discussed in the following paragraphs.

The problem of a small, single, heated cylinder placed normally to a fluid stream has been investigated by Giedt[17,18] where he determined the heat transfer coefficients around the cylinder for a Reynolds number range of $7.08\times10^4 \le Re_D \le 2.19\times10^5$. The size and geometry of the test hardware used in this investigation were markedly different from that in the present study where the geometry was composed of three large cylinders (ET and two RSRMs) and a triangular plate (Orbiter wing) as shown in Fig. 3. The RSRM diameter is 36 times larger than the small 4-in. cylinder used in Giedt's experiment. This means that in order to achieve equivalent Reynolds numbers in the flow around the RSRMs and Giedt's cylinder, the velocity used in the present study would have had to have been decreased 36 times assuming constant viscosity. This means that the condition of dynamic similarity would not have been fully satisfied. Under conditions of low wind velocities and large cylinder diameters, the problem is not one of pure forced convection but rather, a case where forced and natural convection coexist and thus must be treated simultaneously.

Hilpert[17,18] found that the average Nusselt number for gases flowing normal to single cylinders could be represented by an empirical relation of the form

$$\overline{Nu}_D = \bar{h}D/k_f = CRe_D^m\, Pr^{1/3} \tag{7}$$

where C and m are functions of the Reynolds numbers.

In a more recent, alternative correlation by Zhukauskas,[17] the average Nusselt number takes the form

$$\overline{Nu}_D = \bar{h}D/k_f = CRe_D^m\, Pr^{n1}\, (Pr_\infty/Pr_s)^{1/4} \tag{8}$$

where the Prandtl and Reynolds numbers ranges are $0.7 < Pr < 500$ and $1 < Re_D < 10^6$ and where all properties are evaluated at the freestream temperature, except Pr_s which is evaluated at the cylinder surface temperature. Values of C and m are again functions of Re_D and the exponent $n1$ is a function of Pr such that if $Pr \le 10$, $n1 = 0.37$ and if $Pr > 10$, $n1 = 0.36$.

Generally, the average Nusselt number for a gas flowing normal to a single smooth cylinder can be represented by the following equation[19]:

$$\overline{Nu}_D = \bar{h}D/k_f = CRe_D^m Pr^{n1} + \overline{Nu}_{D,NC} \tag{9}$$

In this equation, the velocity used in computing the Reynolds number is that of the gas stream approaching the cylinder. All fluid properties are evaluated at the film temperature. The coefficient C and exponents m and $n1$ are functions of the Reynolds number Re_D and of the Prandtl number Pr, respectively. As the Reynolds number approaches zero, the Nusselt number reduces to the Nusselt number ($\overline{Nu}_{D,NC}$) for natural convection.

Ahmad[20] investigated the free and forced convection from a horizontal cylinder in crossflow of air having a uniform heat

Table 1 Forced convection heat transfer coefficients for cylinders in crossflow

Equation	C	m	$n1$	$\overline{Nu}^a_{D,NC}$	Range of Re_D	$\overline{Nu}_D$	$\bar{h}^b$	Reference
—	—	—	—	—	5.17×10^6	3874	4.29	Present
7	0.027	0.805	0.33	0	$4.0\times10^4 - 4.0\times10^5$	6141	6.87	17,18
8	0.076	0.700	0.37	0	$2.0\times10^5 - 1.0\times10^6$	3367	3.76	17
9	0.021	0.814	0	0	$5.0\times10^4 - 2.0\times10^5$	6124	6.85	19
9	0.328	0.56	0	0	$8.0\times10^3 - 1.0\times10^5$	1886	2.11	19
9	0.270	0.60	0	0	$6.0\times10^3 - 1.3\times10^5$	2880	3.22	19
9	0.157	0.64	0	0	$5.0\times10^3 - 4.2\times10^5$	3108	3.48	19
9	0.500	0.54	0	0	$3.9\times10^4 - 1.1\times10^5$	2110	2.36	19
9	0.143	0.67	0	0	$2.0\times10^4 - 1.2\times10^5$	4502	5.03	19
9	0.150	0.67	0	0	$3.0\times10^4 - 1.2\times10^5$	4722	5.28	19
9	0.380	0.56	0	0	$4.0\times10^4 - 1.3\times10^5$	2184	2.74	19
9	0.063	0.72	0	0	$1.3\times10^5 - 3.0\times10^5$	4296	4.80	19
9	0.360	0.58	0	0	$5.7\times10^4 - 1.2\times10^5$	2819	3.15	19
9	0.185	0.62	0	0	$1.0\times10^3 - 2.0\times10^5$	2689	3.01	19
9	0.510	0.50	0	0	$7.0\times10^2 - 5.0\times10^4$	1160	1.30	19
9	0.023	0.80	0	0	$>5.0\times10^4$	5402	6.04	19
9	0.197	0.60	0	0	$5.0\times10^3 - 5.0\times10^4$	2102	2.35	19
9	0.330	0.60	0.33	0	—	3156	3.53	19
10	0.067	0.733	0	0	$6.8\times10^3 - 2.1\times10^4$	5586	6.24	20
11	—	—	—	—	—	—	11.55	21
—	—	—	—	—	3.96×10^6	5890	6.95	22

[a]Neglected compared to the Nusselt number of forced convection. [b]Btu/h-ft²°F.

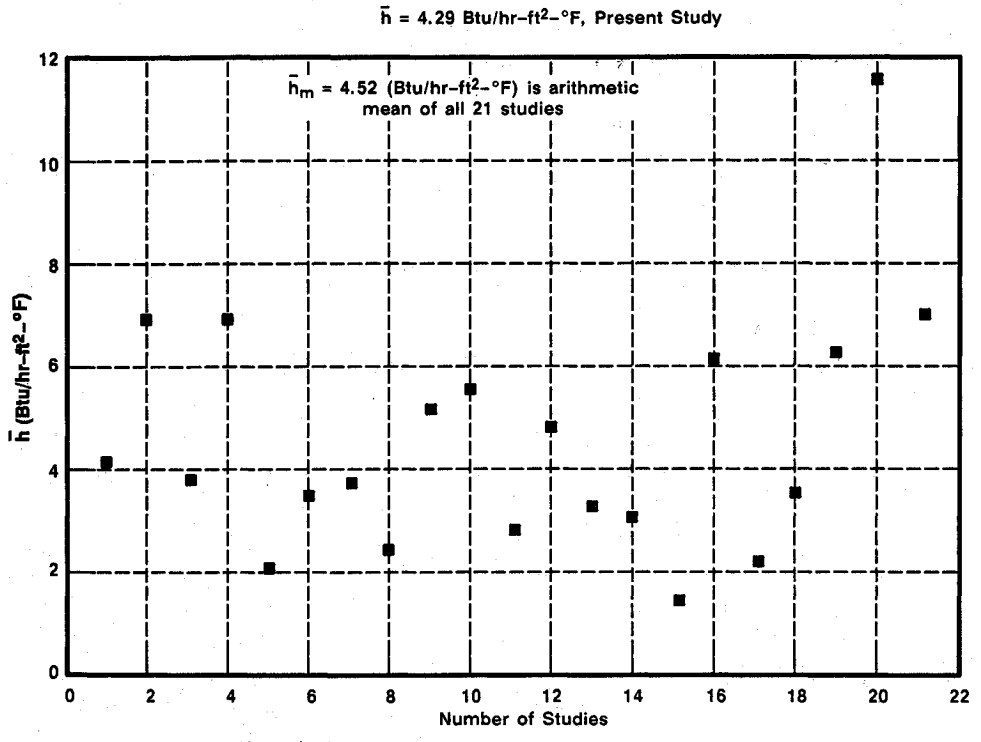

Fig. 7 Average forced convection heat transfer coefficient for cylinders in crossflow.

flux boundary condition at the surface. Tests were conducted in a low speed open-circuit wind tunnel. The average Nusselt number in the forced convection regime ($6{,}800 \leq Re_D \leq 21{,}300$) was correlated by the equation

$$\overline{Nu}_D = \bar{h}D/k_f = 0.0675\ (Re_D)^{0.7333} \tag{10}$$

Results from applying the correlations given in Eqs. (7-10) to calculate the average heat transfer coefficient are shown in Table 1. Included and shown as the first entrant in the table is the heat transfer coefficient (4.29 Btu/h-ft²-°F) and the Nusselt number (3874) as calculated for the west RSRM in the present study for the more realistic case where radiation to the sky was considered. For this case, the average west RSRM surface temperature was 24°F. The west RSRM was selected because the northwest wind impinges directly upon this motor and therefore it affords a more appropriate comparison with the results predicted by the correlations.

The Reynolds number (5.17×10^6) shown for the present study was calculated using the freestream velocity approaching the STS (58 ft/s), the diameter of the RSRM (12.2 ft), and a kinematic viscosity value for air based on a film temperature, which was the average of the computed surface temperature (24°F) and the ambient temperature (15°F) used in the study. It should be noted that this Reynolds number, although generally larger than the upper limit on the range of Reynolds number applicability, was arbitrarily used in each of the correlations so that a direct comparison of the predicted values from Eqs. (7-10) could be made with the PHOENICS '81 result. Using this Reynolds number, the coefficient C and exponents m, $n1$ for each correlation were determined from the appropriate reference, and the average Nusselt number was calculated. Then, the average heat transfer coefficient was calculated from the definition of the average Nusselt number.

References 21 and 22 describe experimental studies to determine the forced convection heat transfer coefficient. Reference 21 describes an experiment which was conducted to determine the forced convective heat transfer coefficient at the surface of an uninsulated cylindrical tank filled with liquid oxygen. The tank was 18 in. in diameter and 22 ft high with a 0.094 in. thick wall of 304 stainless steel. The average convective heat transfer coefficient was found to be

$$\bar{h} = 0.355\ (X + 1.6)/\ D_o^{0.195}\ [U_\infty/(X - 0.712)]^{0.805} \tag{11}$$

where D_o is the outside cylinder diameter (ft) with $D_o = 1.5$ ft for values of $D_o > 1.5$ ft, U_∞ is the wind velocity (knots), and X is the ambient air temperature in $°R/100$. This correlation suggested a possible application to the large STS cylindrical components. However, when the values ($T_\infty = 15°$F, $U_\infty = 58$ ft/s = 34.33 knots) from the present study were used in this expression, along with $D_o = 1.5$ ft, the average heat transfer coefficient was calculated to be 11.55 Btu/h-ft²-°F, which is much larger than all other values of Table 1. This is believed to be due to the absence of insulation or a limitation on the use of this correlation to situations where the wind speed is much less than the 58 ft/s velocity used in this study, or both.

Reference 22 describes an experimental study conducted during the SRM redesign, which provides a test data point. The three RSRM case field joints are maintained at a specified temperature with electrical heaters. To certify[9] the capability of a 3.5 kW heater to heat and maintain the O-rings within a joint at the required 75°F temperature for an ambient temperature of 20°F and a 40 mph wind, tests were conducted on a section of the full motor segment. The 12-ft-diam, 12-ft-high section containing a joint and a heater was placed between two walls to provide a 2-ft clearance on either side of the section and the adjacent wall. An enclosed airplane propeller placed 20 ft upstream of the section generated a 28 mph wind, which resulted in an approximate 40 mph local wind condition in the venturi between the section and the walls. The local heat transfer coefficient at the forward stagnation point was calculated to be 5.1 Btu/h-ft²-°F from the measured data; this increased with increasing distance from the stagnation point due to the venturi effect. An average heat transfer coefficient of 6.95 Btu/h-ft²-°F was found for the RSRM surface. This value is larger than the predicted value of 4.29 Btu/h-ft²-°F but is thought to be acceptable in view of the difference between the test configuration and that considered in this study.

Figure 7 shows the 21 predicted values ($n = 21$) of the average heat transfer coefficient as given in Table 1. They vary from 1.31 to 11.55 Btu/h-ft^2-°F giving a mean value (h_m) of 4.52 Btu/h-ft^2-°F and a biased standard deviation (σ') of 2.34 Btu/h-ft^2-°F. In the present study, the calculated average circumferential value of the west RSRM surface heat transfer coefficient was 4.29 Btu/h-ft^2-°F which is 5.1% less than the mean value. Based upon an application of the Student's t distribution,[23] the very large value of 11.55 Btu/h-ft^2-°F can be excluded with 99.5% confidence. When this is done, the resulting mean value becomes 4.17 Btu/h-ft^2-°F, and the biased standard deviation is 1.74 Btu/h-ft^2-°F. The calculated average value of the RSRM heat transfer coefficient is now 2.8% larger than the mean value. The dispersion of values shown in Fig. 7 can be attributed to a variety of factors[19] associated with the experiments or the theory.

At this point, a tolerance analysis was conducted to determine what the upper and lower limits of the average heat transfer coefficient would have to be for this dispersed region such that there is a 90% confidence that at least 99.73% of all coefficients lie within these limits. The analysis was done assuming a normal distribution of all of the coefficients within the reduced population ($n = 20$) and using the mean ($h_m = 4.17$ Btu/h-ft^2-°F) and biased standard deviation ($\sigma' = 1.74$ Btu/h-ft^2-°F) values already calculated. The upper ($\bar{h}_u$) and lower ($\bar{h}_l$) limits were determined in terms of h_m, σ', and K where K is a statistical variable dependent upon the population size. The limits are defined as $\bar{h}_u = \underline{h}_m + K\sigma'$ and $\bar{h}_l = h_m - K\sigma'$. In this case where $K = 3.922$, $\bar{h}_u = 11.010$ Btu/h-ft^2-°F and $\bar{h}_l = -2.674$ Btu/h-ft^2-°F. Since a negative heat transfer coefficient is physically meaningless, realistically $\bar{h}_l = 0$. Based on this analysis, one can conclude that, even with an increased population size as a result of additional experiments, one can be 90% confident that the heat transfer coefficient will be less than 11.010 Btu/h-ft^2-°F.

The above experimental study[22] yielded information on the stagnation point heat transfer for a large cylinder. Van Driest[18] has recommended the following correlation for calculating the Nusselt number for incompressible airflow at the forward stagnation point on cylinders

$$Nu_{D,fsp} = 1.0427 Re_D^{1/2} \tag{12}$$

where the fluid properties are evaluated at the mean film temperature and the Reynolds number is based on the freestream velocity. In this study, the forward stagnation point on the west RSRM was in line with the assumed northwest wind direction. For case 2, with thermal radiation to the sky, the calculated local Nusselt number for the west RSRM at its forward stagnation point ($\theta = 150$ deg) was 3800. Using the freestream Reynolds number of 5.17×10^6, Eq. (12) yields a value of 2371. This difference may be due to the fact that the local Reynolds number for the cell at the forward stagnation point in the present analysis was higher than the freestream Reynolds number. Other possible reasons for the difference may be the radiation to the sky, the use of stepped walls when using Cartesian coordinates, and surface irregularities. It is well known that roughening of the surface can considerably enhance heat transfer, especially with forced convection.

Correlations relating to the stagnation point heat transfer include that of Schlichting.[24] His expression for the local Nusselt number at the forward stagnation point is similar to that of Van Driest[18] and is

$$Nu_{D,fsp} = C_1 Re_D^{1/2} \tag{13}$$

when Reynolds numbers are in the range $0.76 \times 10^5 \leq Re_D \leq 1.7 \times 10^5$ and where C_1 increases as Re_D increases. Also Squire[25] has solved the equations of motion and energy for a cylinder at constant temperature in crossflow of air for that portion of the cylinder to which a laminar boundary layer adheres. He has shown that at the forward stagnation point and in its immediate neighborhood,

$$Nu_{D,fsp} = 1.00 Re_D^{1/2} \tag{14}$$

The wide dispersion in the published correlations relating to heat transfer from smooth cylinders can be attributed, as already stated, to various factors associated with the experiments or the theory. Aside from these factors, their use in this study was avoided since the correlations were generally developed for small, single cylinders and not for a grouping of large cylinders as typified by the STS. Thus there was some question concerning the appropriateness of the correlations. Table 1 shows the values of the average heat transfer coefficient determined from these correlations as well as those determined from the experimental studies and the analyses. The value (4.29 Btu/h-ft^2-°F) obtained from the PHOENICS '81 solution is believed to most realistically represent the heat transfer coefficient at the surface of both RSRMs but particularly for the west RSRM under the worst wintertime conditions. It is consistent with the 3°F ET chilling effect determined in this study.

Conclusions

The PHOENICS '81 solution is believed to provide the most accurate flow/thermal description of the STS launch pad environment after the ET has been filled and under the severest of winter conditions.

From the PHOENICS '81 solution, the temperature depression or the chilling of the air in the pad environment was calculated to be 3°F relative to the ambient. This compares with a 1–2°F RSRM surface temperature depression as obtained from the prelaunch temperature measurements on the winter flight of STS-29. Since RSRM surface temperatures would normally be slightly higher than the temperature of the local air adjacent to a surface, the predicted temperature depression appears to be substantiated. The difference between the predicted and the STS-29 derived values of the temperature depression could possibly be attributed to other factors. These include the more severe ambient temperature (15°F) assumed in the present analysis than the actual average ambient temperature (59°F) existing prior to and at the time of the launch of STS-29.

Acknowledgments

This study was supported by the NASA Marshall Space Flight Center, under Contract NAS8-30490. The authors wish to thank other members of the Aero/Thermal Section of Thiokol for helpful discussions and suggestions.

References

[1]Anon., "Thermal Modeling of the Space Shuttle Launch Configuration," SRS Technologies, Huntsville, AL, SRS/STD-TR86-022, 604a, Final Rept., 1986.

[2]Singhal, A. K., Tam, L. T., Bachtel, F., and Vaniman, J., "Thermal Environment Around the Space Shuttle With Hot-Gas Jets for Ice Suppression," *Journal of Spacecraft and Rockets*, Vol. 23, No. 6, Nov.–Dec. 1986, pp. 547–553.

[3]Bachtel, F., "Shuttle Pad Environments," NASA Marshall Space Flight Center, Huntsville, AL, July 1987.

[4]Hughes, J. T., and Wilson, M. E., "Space Shuttle Program Thermal Interfaces Design Data Book," Rockwell International, Downey, CA, Rept. SD 74-SH-0144E, Dec. 1987, pp. 2–69, 2–74.

[5]Mongan, R., "TIDDB Prelaunch Verification Status Review Meeting," Downey, CA, Aug. 10, 1987.

[6]Gunton, M. C., Rosten, H. I., Spalding, D. B., and Tatchell, D. G., "PHOENICS an Instruction Manual," CHAM of North America, Huntsville, AL, TR/75, 1983.

[7]Singhal, A. K., and Owens, S. F., "Introduction to PHOENICS," CHAM of North America, Huntsville, AL, Feb. 1984.

[8]Ahmad, R. A., "Plans Associated with the Flow and Thermal Fields Around the STS," Morton Thiokol, Brigham City, UT, Interoffice Memo L213-FY87-M089, April 1987.

[9]Anon., "CEI Specification," Morton Thiokol, Brigham City, UT, CPW1-3600A, Paragraph 3.2.1, Paragraphs 3.2.7.1a1, 3.2.7.1a2, 3.2.7.1a3, 3.2.1.11a, Aug. 1987.

[10]"Space Shuttle Flight and Ground System Specification, Natural Environment Design Requirements," National Space Transportation System, NASA, NSTS 07700, Vol. 10, Appendix 10.10, April 1987, pp. 3, 4.

[11]Maw, J. F.,"STS-51L RSRM Grain and O-Ring Temperature Calculations, Action Item 2-18-001," Morton Thiokol, Brigham City, UT, TWR-300014, Feb. 1986.

[12]"Space Shuttle External Tank, Thermal Data Book," Martin Marietta, Michoud Div., New Orleans, LA, June 1981.

[13]"Documentation of Convective CFD Analytical Support to the TIDDB Verification," Rockwell International, Huntsville, AL, No. 112-041-B11-01, Oct. 1987.

[14]"Report of the Presidential Commission on the Space Shuttle Challenger Accident," Washington, DC, June 1986, p. 62.

[15]Ahmad, R. A., and Tran, T. M., "External Flow and Thermal Fields Around the Space Shuttle on the Launch Pad," Morton Thiokol, Brigham City, UT, TWR-16766, June 1987.

[16]Ahmad, R. A., and Tran, T. M., "External Flow and Thermal Fields Around the Space Shuttle on the Launch Pad," Morton Thiokol, Brigham City, UT, TWR-16766, Rev. A, Nov. 1987.

[17]Incropera, F. P., and Dewitt, D. P., *Introduction to Heat Transfer*, Wiley, New York, 1985, Chap. 7.

[18]Chapman, A. J., *Heat Transfer*, 3rd ed., Macmillan, 1974, Chap. 8.

[19]Morgan, V. T., "The Overall Convective Heat Transfer From Smooth Circular Cylinders," *Advances in Heat Transfer*, Vol. 11, 1975, pp. 199–264.

[20]Ahmad, R. A., "Mixed Convection Around a Horizontal Cylinder," Ph.D. Thesis, University of Illinois, Chicago, 1985.

[21]Anon., "Atmospheric Heat Transfer to Vertical Tanks Filled with Liquid Oxygen," Arthur D. Little, Cambridge, MA, Special Rept. 50, Nov. 1958.

[22]Buttars, R. L., "Thermal Analysis/Verification of Morton Thiokol RSRM Joint Heater Design," Morton Thiokol, Brigham City, UT, TWR-16097, 1987.

[23]Mendenhall, W., *Introduction to Probability and Statistics*, 4th ed., Duxbury Press, 1975, Chap. 9

[24]Schlichting, H., *Boundary Layer Theory*, 7th ed., McGraw-Hill, New York, 1979, Chap. 12.

[25]Kreith, F., *Principles of Heat Transfer*, 2nd ed., International Textbook, 1965, Chap. 9.

Paul F. Mizera
Associate Editor